Stick-slip suppression and speed tuning for a drill-string system via proportional-derivative control

Wei Lin[a], Joseph Páez Chávez[b,c], Yang Liu[d,*], Yingxin Yang[a], Yuchun Kuang[a]

[a]*School of Mechatronic Engineering, Southwest Petroleum University, Chengdu, 610500, China*
[b]*Mathematical Institute, University of Koblenz-Landau, Universitätstr. 1, D-56070 Koblenz, Germany*
[c]*Center for Applied Dynamical Systems and Computational Methods (CADSCOM), Faculty of Natural Sciences and Mathematics, Escuela Superior Politécnica del Litoral, P.O. Box 09-01-5863, Guayaquil, Ecuador*
[d]*College of Engineering Mathematics and Physical Sciences, University of Exeter, North Park Road, Exeter, EX4 4QF, UK*

Abstract

This paper studies the problems of stick-slip mitigation and speed tuning for a lumped-parameter drill-string system by using a proportional-derivative feedback controller via path-following analysis. In this study, we consider two main control parameters, the weight-on-bit and the desired drill-bit speed, which in general differs from the real angular speed. In particular, we determine the combinations of these two parameters for which the proposed control scheme is applicable, which is affected by the non-smooth nature of the system induced by bit-rock interaction. Our analysis using path-following techniques for non-smooth systems reveals the inherent coexistence of stick-slip vibration and constant rotation, and identifies a critical point where the drill-bit speed coincides with the desired angular speed. Furthermore, our analysis proposes a strategy that allows controlling the drill-bit speed to suppress stick-slip, by tuning the controller in a suitable manner.

Keywords: Drill-string; Stick-slip; Non-smooth dynamical system; Numerical continuation; Coexisting attractors

1. Introduction

In oil and gas drilling, the drill-string system shown in Fig. 1 includes a rotary table, a series of hollow drill pipes, several relatively thicker drill collars, and a drill-bit. It is essentially used to transfer torque from the rotary table on the surface to the drill-bit in borehole, and generally can run up to several kilometres deep [1]. Such a long and slender structure makes drilling process susceptible to the stick-slip phenomenon, a self-excited torsional vibration [2–4]. Stick-slip vibrations decrease drilling efficiency, degrade borehole quality, provoke premature drill-bit wear, and cause drill-string failures. In practice, these vibrations exist in the 50% of drilling time [5] causing drill-bit to whip and rotate at a high speed, which can lead to severe bit bouncing phenomenon and whirl motion at the bottom hole assembly (BHA), see Fig. 1(a). The term of bit bouncing refers to axial vibrations of the drill-bit leading to loss of contact between the bit and the drilled medium, while whirl motion is due to drill pipe eccentricity producing lateral vibrations. In this work, our main focus will be on mitigation of stick-slip vibrations and development of effective control strategies for this purpose.

In the present work, we will study the mitigation of stick-slip vibrations by using a proportional-derivative (PD) controller via numerical continuation methods. Mitigation of torsional stick-slip vibrations has received considerable attention in the past, with a large number of both analytical and experimental studies [7–12]. In general, there are passive and active control strategies. Passive control strategies [13] utilise the internal structures of the drill-strings to mitigate stick-slip vibrations, such as optimization of BHA configuration, drill-bit selection and optimum design [14], as well as utilization of anti stick-slip tools [15, 16]. Active control strategies concerns the use of a certain actuation mechanism

*Corresponding author. Tel: +44(0)1392-724654, e-mail: y.liu2@exeter.ac.uk.

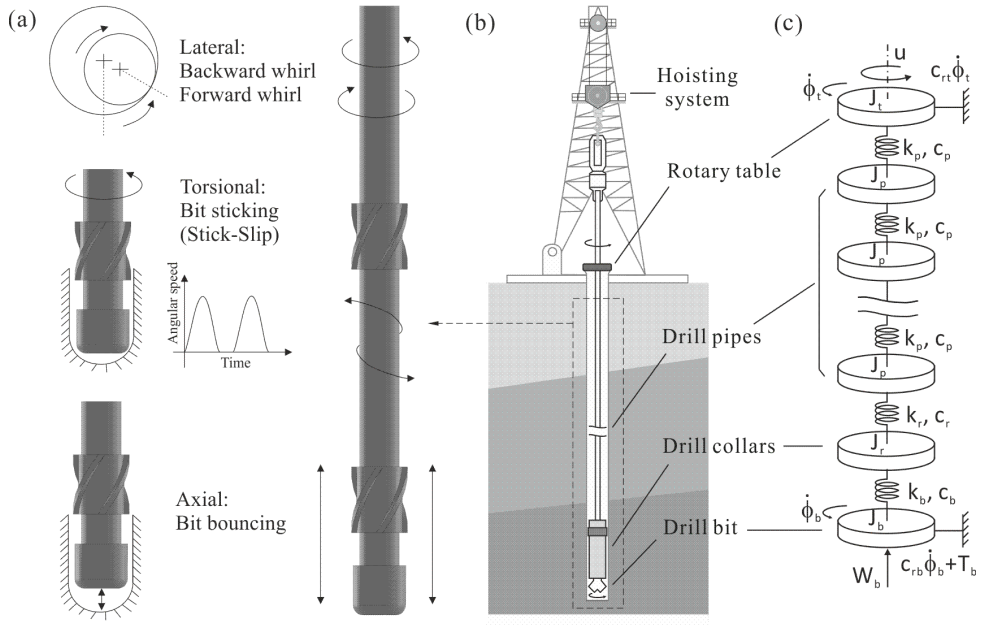

Figure 1: (a) Lateral, torsional and axial vibrations encountered in drill-strings during operation [6], and schematics of (b) an oilwell drilling rig and (c) a simplified physical model of the drill-string.

(via external energy) driven by feedback signals related to the actual drill-bit speed or angular position. Our studies in this paper will focus on active control using the feedback information of drill-bit and rotary table. Until now, many feedback control approaches have been developed to mitigate torsional stick-slip vibrations. For example, Canudas-de-Wit *et al.* developed a novel weight-on-bit (WOB) control law leading the drill-string to a globally asymptotically stable closed-loop system [17]. The WOB control strategy can greatly decrease the rate of penetration. Navarro-López and Licéaga-Castro investigated the stick-slip vibrations of a discontinuous lumped-parameter drill-string model by studying its stability characteristics at different system equilibria [18]. In particular, bifurcation analyses considering WOB and rotary speed as the branching parameters were carried out by using the software package AUTO [19], a bifurcation analysis tool for smooth dynamical systems. This software tool allows to a great extent the study of constant rotation regimes of the considered drill-string model, but results of this type concerning stick-slip motion are rather limited. In this work, we will employ the continuation platform COCO [20, 21], which implements numerical routines for the study of bifurcation problems of both smooth and non-smooth dynamical systems. In this way, COCO will be used to carry out an in-depth parametric investigation of stick-slip vibrations, which involves the numerical treatment of piecewise-smooth periodic solutions. Furthermore, Liu studied a sliding mode control strategy to avoid undesired bit sticking and stick-slip vibrations while tracking a desired angular speed [22]. Karkoub *et al.* used the $\mu-$synthesis control design technique allowing the inclusion of modelling errors in terms of uncertain weights [23]. However, this drill-string model is required to be linearized around its operating point in order to apply the $\mu-$synthesis technique. So, the performance of the controller cannot be guaranteed if more degrees of freedom of the system are considered. On the other hand, Ritto *et al.* proposed different PD control strategies and constructed a torsional stability map to study the performance of these PD controllers [24]. Vromen *et al.* developed an observer-based output-feedback controller which was verified through realistic drilling case studies [25, 26]. From a control point of view, an important issue that deserves attention is the determination of system parameter ranges for which the applied control strategy is effective, specially in terms of the stability of the desired system response. In particular, it has been observed that the desired drill-bit speed is not always achievable for a specific control method due to the nonlinearity of bit-rock interaction, and therefore suitable ranges where the controller can operate effectively should be identified. As mentioned above, all of the controllers were proposed for mitigating stick-slip

vibrations, but the exact speed control and the hidden multistable dynamics of the drill-string system have not been studied yet. In this work, we will pay particular attention to these issues and study the proposed controller by considering the desired drill-bit speed and weight-on-bit in terms of the actual angular speeds and stick-slip mitigation.

Another goal of the present paper is to study the multistability of the drill-string system under the action of the proposed controller, as well as to investigate the evolution of the resulting coexisting attractors. In [4], three attractors of the system, including friction-induced torsional stick-slip vibrations, constant rotation, and permanent bit sticking, have been observed to coexist within a certain parameter window, and this feature was used to steer the response of the system from a sticking equilibrium or stick-slip regime to an equilibrium with constant drill-bit rotation. As is usual in the literature, the drill-string system is modelled by a non-smooth dynamical system, where the near-grazing dynamics (i.e. transitions between stick-slip and no stick-slip oscillations characterized by grazing-sliding bifurcations) and friction-induced vibrations are known to produce rich complex dynamics, such as the appearance of coexisting attractors [27], which could cause catastrophic drill-string failures. To avoid such failures, we will employ a recently developed control method which has been used to control a multistable impact oscillator [28]. Our proposed control scheme is achieved by coupling systems via a linear feedback consisting of the relative angular position and speed of the drill-string. In particular, we will pay special attention to investigating how the proposed controller can be used to effectively drive the system to a desired rotary speed, and furthermore, how to reduce at the same time the severity of stick-slip vibrations.

The contribution of the present paper is trifold: first, studying the hidden bistable dynamics of the drill-string system under a PD controller, and second, determination of the minimum controllable rotary speed for the PD controller, and third, a numerical approach based on path-following techniques for tuning the rotary speed of the system to a desired speed. Our work in this paper is based on a well-established drill-string model, which has been studied by [17, 18, 25, 26] and was validated using field data by [24]. The drill-strings are simplified by a torsional model. It consists of four elements: (1) the rotary table system (J_t), (2) the drill pipes (J_p), (3) the drill collars (J_r), (4) the drill bit (J_b). The drill pipes are much more longer than other components. Therefore, the drill pipes are usually divided by more elements. The elements are connected one to each other by linear springs with torsional stiffness k_p, k_r, k_b and torsional damping c_p, c_r, c_b. A viscous damping is considered at the rotary table system c_{rt} and at the bit c_{rb}. A friction torque T_b is considered acting at the bit. The model only considers torsional vibrations of drill-strings without consideration of axial vibration coupling. However, the axial vibration could be taken into account by varying the WOB periodically, but this is not the main focus of this study. The main contributions of this work are twofold: first, studying multistability in drill-strings when rotary speed is low, and second, a numerical approach based on path-following techniques that allows controlling rotary speed and stick-slip mitigation by tuning the PD controller in a suitable manner.

The remainder of the paper is organized as follows. In Section 2, the physical model and equations of motion of the drill-string system are introduced, as well as the mathematical formulation of the proposed controller. In Section 3, the dynamical behaviour of the drill-string model under the action of the proposed control law is analyzed via numerical continuation methods. Our study starts with the one-parameter analysis without and with consideration of the proposed controller, which is followed by a two-parameter analysis. The severity of stick-slip vibrations is also investigated under the variation of different control parameters. Finally, the main conclusions of the present work are given in Section 4.

2. Mathematical model of the lumped-parameter drill-string system

In this section we will analyze the dynamical behaviour of the drill-string shown in Fig. 1 (a) under the action of a PD controller. Fig. 1 (b) shows a physical representation of a lumped-parameter system based on a series of disks interconnected via torsional springs and dampers. Specifically, the model considers a number of disks, corresponding to the rotary table (t), drill-pipes (p), drill collars (r) and drill-bit (b). In this study, we will consider one drill pipe in the drill-string model. Therefore, in this setting the mathematical description of the generalized lumped-parameter model can be divided into two operation modes (*Stick* and *Slip*), as follows. It should be noted that this model has been developed and used in [4, 6], and we will briefly introduce it here for studying the proposed PD controller. It is

also worth noting that Liu *et al.* studied the stick-slip oscillations encountered in the model from both numerical and experimental points of view [4]. Liu *et al.* focused on analysing the cause of coexistence of sticking, stick-slip vibration, and constant rotation in the model [6]. Different from [4, 6], this paper studies a numerical approach based on path-following techniques which allows controlling rotary speed of the drill-string and stick-slip mitigation by using a newly developed PD controller.

Slip (SL). In this mode the drill-bit rotates with positive angular speed, and the system motion is governed by the equations

$$\begin{cases} J_t\ddot{\phi}_t + c_{rt}\dot{\phi}_t + c_p(\dot{\phi}_t - \dot{\phi}_p) + k_p(\phi_t - \phi_p) = u, \\ J_p\ddot{\phi}_p + c_p(\dot{\phi}_p - \dot{\phi}_t) + c_r(\dot{\phi}_p - \dot{\phi}_r) + k_p(\phi_p - \phi_t) + k_r(\phi_p - \phi_r) = 0, \\ J_r\ddot{\phi}_r + c_r(\dot{\phi}_r - \dot{\phi}_p) + c_b(\dot{\phi}_r - \dot{\phi}_b) + k_r(\phi_r - \phi_p) + k_b(\phi_r - \phi_b) = 0, \\ J_b\ddot{\phi}_b + c_{rb}\dot{\phi}_b + c_b(\dot{\phi}_b - \dot{\phi}_r) + k_b(\phi_b - \phi_r) + T_b^{\mathrm{SL}} = 0. \end{cases} \tag{1}$$

where ϕ_t, ϕ_p, ϕ_r, and ϕ_b are the angular positions of the lumped mass, and J_t, J_p, J_r, and J_b are the moments of inertia. c_p, c_r, and c_b are the damping coefficients, and k_p, k_r, and k_b are the torsional stiffness of the drill pipe, drill collar, and drill-bit, respectively. A viscous damping torque, $c_{rt}\dot{\phi}_t$, is considered in this model which corresponds to the lubrication of the mechanical elements of the rotary table, where c_{rt} is a viscous damping coefficient. A viscous damping torque, $c_{rb}\dot{\phi}_b$, is considered on the drill-bit representing the influence of drilling fluids. u is the control torque input, and T_b^{SL} is the reaction torque computed as

$$T_b^{\mathrm{SL}} = \begin{cases} T_0, & \dot{\phi}_b = 0, \\ R_b W_b \left(\mu_{cb} + (\mu_{sb} - \mu_{cb}) e^{-\gamma_b \frac{\dot{\phi}_b}{v_f}} \right), & \dot{\phi}_b > 0, \end{cases} \tag{2}$$

In the expression above, $T_0 = \mu_{sb} R_b W_b$ is the break-away torque, μ_{cb}, μ_{sb} are the Coulomb and the static friction coefficients, respectively, $0 < \gamma_b < 1$ is a constant defining the speed decrease rate, v_f is a speed constant, R_b is the bit radius, and W_b is the WOB. This operation mode terminates at some $t = t_{\mathrm{stick}} \geq 0$ when the angular speed of the drill bit becomes zero, i.e. $\dot{\phi}_b(t_{\mathrm{stick}}) = 0$. At this time, the system switches to the stick mode of operation defined below.

Stick (ST). During this regime the drill-bit is in stationary position, and the system motion is described by the equations

$$\begin{cases} J_t\ddot{\phi}_t + c_{rt}\dot{\phi}_t + c_p(\dot{\phi}_t - \dot{\phi}_p) + k_p(\phi_t - \phi_p) = u, \\ J_p\ddot{\phi}_p + c_p(\dot{\phi}_p - \dot{\phi}_t) + c_r(\dot{\phi}_p - \dot{\phi}_r) + k_p(\phi_p - \phi_t) + k_r(\phi_p - \phi_r) = 0, \\ J_r\ddot{\phi}_r + c_b\dot{\phi}_r + c_r(\dot{\phi}_r - \dot{\phi}_p) + k_r(\phi_r - \phi_p) + k_b(\phi_r - \phi_b) = 0, \\ \ddot{\phi}_b = 0, \quad \dot{\phi}_b = 0. \end{cases} \tag{3}$$

During this mode, the reaction torque is computed via Newton's third law as follows

$$T_b^{\mathrm{ST}} = c_b\dot{\phi}_r + k_b(\phi_r - \phi_b), \tag{4}$$

which means that the reaction torque adjusts itself to enforce the equilibrium with the external torque acting on the drill-bit. This mode terminates at some $t = t_{\mathrm{slip}} \geq 0$ when $T_b^{\mathrm{ST}}\big|_{t=t_{\mathrm{slip}}} = T_0$. At this point, the reaction torque has reached the break-away torque value T_0, where the drill-bit begins to rotate, hence switching the system to the slip phase introduced previously.

For the purpose of mitigating stick-slip vibrations and controlling the drill-bit speed, we propose the following PD controller:

$$u = k_1(\phi_t - \phi_b) + k_2(\Omega_d - \dot{\phi}_t) + k_3(\Omega_d - \dot{\phi}_b), \tag{5}$$

where Ω_d is the desired rotary speed, while the parameters k_1, k_2 and k_3 represent control gains to be adjusted. It should be noted that, in practice, real-time downhole measurement of drill-bit rotation is not

possible. However, this measurement can be estimated by using observer-based state-feedback approach, e.g. [25]. Therefore, we assume the angular position and speed of the drill-bit, ϕ_b and $\dot{\phi}_b$, are measurable in this work.

In order to numerically study periodic and equilibrium solutions of the drill-string model (1)–(4), it is convenient to introduce the following variable transformation

$$\begin{cases} x_t = \phi_t, \\ y_t = \omega_t, \\ x_p = \phi_p - \phi_t, \\ y_p = \omega_p, \\ x_r = \phi_r - \phi_p, \\ y_r = \omega_r, \\ x_b = \phi_b - \phi_r, \\ y_b = \omega_b, \end{cases} \tag{6}$$

where ω_t, ω_p, ω_r and ω_b give the angular speed of the rotary table, drill pipe, drill collar and drill-bit, respectively. According to the operation regimes defined above, the equations of motion of the system can be written in compact form in terms of the new variables as follows

$$z' = \begin{cases} f_{\text{ST}}(z,\alpha), & y_b = 0 \text{ and } T_b^{\text{ST}} = c_b y_r - k_b x_b < T_0, \\ f_{\text{SL}}(z,\alpha), & \text{otherwise}, \end{cases} \tag{7}$$

where $\alpha = (J_t, J_p, J_r, J_b, c_{rt}, c_p, c_r, c_b, c_{rb}, k_p, k_r, k_b, R_b, W_b, \gamma_b, \mu_{cb}, \mu_{sb}, \Omega_d, k_1, k_2, k_3) \in \mathbb{R}^{21}$ and $z = (y_t, x_p, y_p,\ x_r, y_r, x_b, y_b)^T \in \mathbb{R}^7$ stand for the parameters and state variables of the piecewise-smooth system, respectively. In the system introduced above, the vector fields f_{ST} (stick) and f_{SL} (slip) are defined as (cf. Eqs. (1), (3) and (6))

$$f_{\text{ST}}(z,\alpha) = \begin{pmatrix} \frac{1}{J_t}\left(\widetilde{u} - c_{rt}y_t + k_p x_p + c_p(y_p - y_t)\right) \\ y_p - y_t \\ \frac{1}{J_p}\left(k_r x_r - k_p x_p + c_p(y_t - y_p) + c_r(y_r - y_p)\right) \\ y_r - y_p \\ \frac{1}{J_r}\left(k_b x_b - k_r x_r - c_b y_r + c_r(y_p - y_r)\right) \\ -y_r \\ 0 \end{pmatrix},$$

$$f_{\text{SL}}(z,\alpha) = \begin{pmatrix} \frac{1}{J_t}\left(\widetilde{u} - c_{rt}y_t + k_p x_p + c_p(y_p - y_t)\right) \\ y_p - y_t \\ \frac{1}{J_p}\left(k_r x_r - k_p x_p + c_p(y_t - y_p) + c_r(y_r - y_p)\right) \\ y_r - y_p \\ \frac{1}{J_r}\left(k_b x_b - k_r x_r + c_b(y_b - y_r) + c_r(y_p - y_r)\right) \\ y_b - y_r \\ \frac{1}{J_b}\left(c_b(y_r - y_b) - c_{rb}y_b - k_b x_b - T_b^{\text{SL}}\right) \end{pmatrix},$$

where $\widetilde{u} = k_1(-x_b - x_r - x_p) + k_2(\Omega_d - y_t) + k_3(\Omega_d - y_b)$, see Eqs. (5) and (6).

3. Path-following analysis of the dynamical response of the controlled drill-string model

In this section we will present a detailed numerical investigation of the dynamical response of the drill-string model (7). For this purpose, we will apply numerical continuation methods for non-smooth dynamical systems, implemented via the continuation platform COCO [20, 21]. The results of the numerical investigation will be presented using the following solution measure

$$M_{\omega_b} = \frac{1}{T_0}\int_0^{T_0} y_b(t)\,dt = \frac{1}{T_0}\int_0^{T_0} \omega_b(t)\,dt, \tag{8}$$

which gives the average angular speed of the drill-bit in the time window $[0, T_0]$, where T_0 is a suitably chosen positive number. In the case of studying periodic orbits, T_0 will correspond to the period of the solution. Similarly, we will consider the value

$$P_u = \frac{1}{T_0} \int_0^{T_0} u(t)^2 \, dt, \tag{9}$$

which measures the power of the control signal employed to drive the drill-string system. To evaluate the performance of the proposed PD controller, we consider the severity factor of stick-slip vibrations defined as

$$S_{ss} = \frac{\omega_b^{max} - \omega_b^{min}}{\Omega_d}, \tag{10}$$

where ω_b^{max} and ω_b^{min} represent the maximum and the minimum angular speeds of the drill-bit after the transients have decayed, respectively. The rationale of using this severity factor is to compare the maximum angular speed with the minimum one when stick-slip vibration is encountered. Therefore, the larger of the difference $\omega_b^{max} - \omega_b^{min}$ is, the more serious of the fluctuation in the drill-strings is. When $\omega_b^{max} - \omega_b^{min} = 0$, it corresponds to constant rotation of the drill-strings without any fluctuation.

When the PD controller is not applied, the drill-string system can exhibit bit sticking, stick-slip vibration, or constant rotation based on the WOB and control torque. Here, our control goal is to mitigate bit sticking and stick-slip vibration and control the drill-string to rotate at a desired rotary speed Ω_d. Drill-string parameters used in our simulations are given as in Table 1, which were adopted from [18].

Parameter	Value	Unit	Parameter	Value	Unit	Parameter	Value	Unit
J_t	910	$\mathrm{kg \cdot m^2}$	c_p	150	$\mathrm{N \cdot m \cdot s/rad}$	μ_{cb}	0.45	
J_p	2800	$\mathrm{kg \cdot m^2}$	c_r	190	$\mathrm{N \cdot m \cdot s/rad}$	μ_{sb}	0.8	
J_r	750	$\mathrm{kg \cdot m^2}$	c_b	180	$\mathrm{N \cdot m \cdot s/rad}$	R_b	0.15	m
J_b	450	$\mathrm{kg \cdot m^2}$	c_{rt}	410	$\mathrm{N \cdot m \cdot s/rad}$	v_f	1	
k_p	700	$\mathrm{N \cdot m/rad}$	c_{rb}	80	$\mathrm{N \cdot m \cdot s/rad}$	ξ	10^{-6}	
k_r	1080	$\mathrm{N \cdot m/rad}$	k_b	910	$\mathrm{N \cdot m/rad}$	γ_b	0.85	
u	-	$\mathrm{kN \cdot m}$	W_b	-	kN	$\omega_t, \omega_b, \Omega_d$	-	rad/s
k_1	-	$\mathrm{N \cdot m/rad}$	k_2, k_3	-	$\mathrm{N \cdot m \cdot s/rad}$	t	-	s

Table 1: Physical parameters of the drill-string system adopted from a real drill-string design [18] and relevant units.

3.1. One-parameter analysis without control

An initial simulation for the drill-string system under variations of the WOB and constant control torque (i.e. taking $u =$ constant, see (5)) is presented in Fig. 2, where all initial values of the variables $(x_t, y_t, x_p, y_p, x_r, y_r, x_b, y_b)$ are chosen at the origin. As can be seen from the figure, three stable states, constant rotation, stick-slip vibration, and bit sticking, can be observed. As the WOB is small, the drill-string system can be maintained at the constant rotation regime of drilling. However, smaller WOB corresponds to a lower rate of penetration of drilling, so a higher WOB is always desired. As the WOB increases, stick-slip vibrations emerge, and the bit could be permanently stuck in borehole due to the increased WOB. It can be seen from the boundaries of stick-slip and bit sticking, increasing the constant control torque will not help to enlarge the regime of constant rotation significantly. It is therefore that in the present work, we propose a control method to enlarge the operating regime for constant rotation.

Next, the dynamical behaviour of the drill-string model under open-loop torque control can be observed in Fig. 3, which is obtained via path-following of the dynamical response of the drill-string model (7) with respect to the control torque u, showing the average angular speed of the drill-bit (see (8)) on the vertical axis. The continuation was started at $u = 0$ when the drill-bit does not rotate (i.e. $\omega_b = 0$). As the control torque gradually increases, the torque applied on the drill-bit increases as well, but it is not enough to bring the drill-bit into rotation, due to the opposing reaction torque. A critical value is

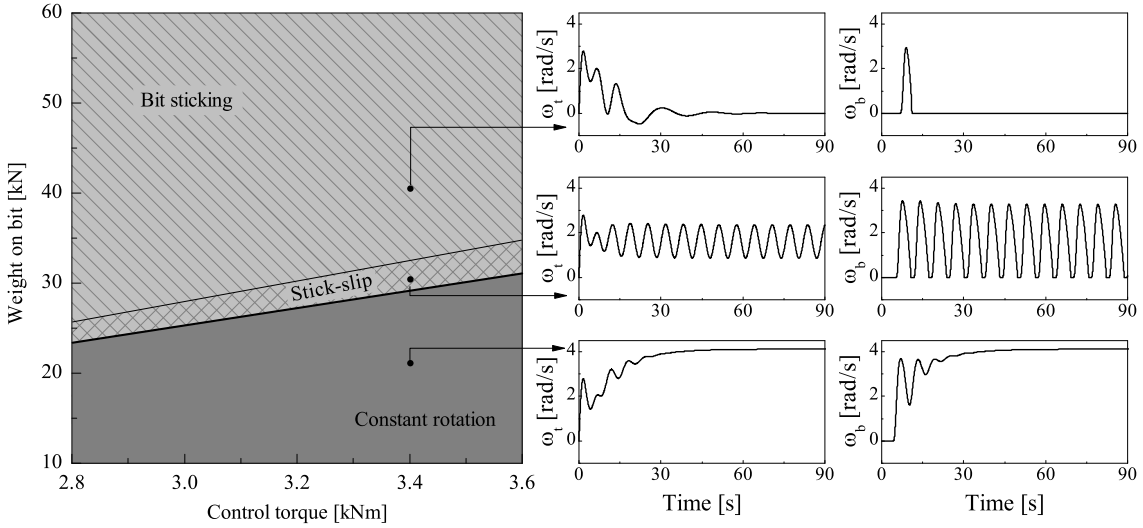

Figure 2: Different operating regimes of the drill-string system without the PD controller under variations of the WOB and constant control torque.

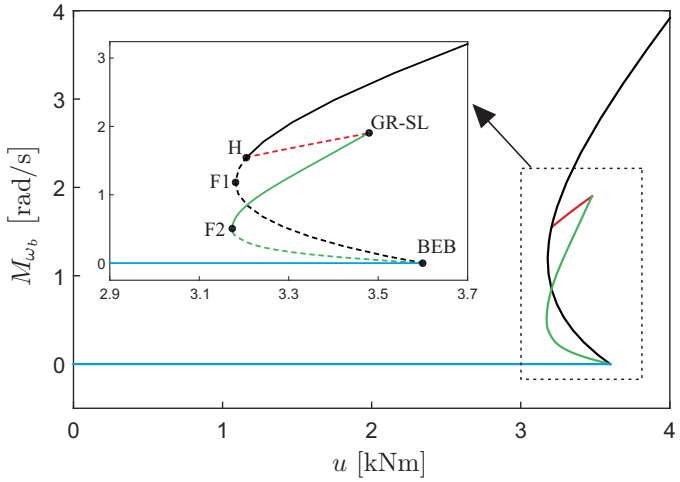

Figure 3: Numerical continuation of the dynamical response of the drill-string model (7) with respect to the open-loop torque control u, computed for the same parameter values of Fig. 2 when $W_b = 30$. The black and blue curves represent the continuation of equilibrium points corresponding to $\omega_b > 0$ (constant rotation) and $\omega_b = 0$ (bit sticking), respectively. The green curve stands for the continuation of stick-slip solutions, while the red branch corresponds to periodic solutions with no sticking phases. Solid and dashed lines denote stable and unstable solutions, respectively. The vertical axis gives the average angular speed of the drill-bit computed via (8).

found when $u = 3.6$, where a *boundary-equilibrium* bifurcation (labeled BEB) takes place, consisting in a situation in which an equilibrium point lies at a discontinuity boundary (see [29]). Such bifurcations can manifest themselves in several ways, for instance as a non-smooth fold, as it is in our case. In this scenario we have that a branch of unstable (dashed black curve) and stable (solid blue curve) equilibria collide at the BEB point, hence resembling the behaviour observed for fold bifurcations of smooth systems.

At the BEB point found before there is an emanating curve (plotted as a dashed green line) of unstable periodic orbits, corresponding to stick-slip solutions. If we decrease the control torque along this curve, we find a critical point $u \approx 3.1736$ (labeled F2) where a fold bifurcation of limit cycles takes place. At this point, the stick-slip solutions become stable, and remain so until the critical point GR-SL is found ($u \approx 3.4788$), where a grazing-sliding bifurcation occurs. Here, a branch of oscillatory unstable

solutions (dashed red curve) with no sticking phases appears, which ends at a subcritical Hopf bifurcation ($u \approx 3.2059$) located on the black curve (equilibria representing constant rotation of the drill-bit).

Fig. 3 represents a practical operation for the drill-string system, where the drill-strings start to rotate from stationary as the control torque from the rotary table increases from zero. When the torque increases to $u \approx 3.1736$ (labeled F2) and $u \approx 3.2059$ (labeled H), the sticking bit could be suddenly switched to the branches of stick-slip and constant rotation, respectively, due to external disturbances, such as pipe-borehole interaction. Unless the control torque increases to $u = 3.6$ (labeled BEB), this multistable regime (between F2 and BEB) is completely avoided and the drill-strings will rotate at a constant speed. In the next subsection, we will study how to use our proposed PD controller to overcome this multistability if the drill-string system is operated in this regime.

3.2. One-parameter analysis with control

In order to mitigate stick-slip vibrations, the proposed PD controller is applied to the drill-string system, and its dynamic response is shown in Fig. 4. As can be seen from the figure, the drill-string system exhibits stick-slip vibrations initially, and the PD controller is switched on at $t = 30$ seconds. Thereafter, the angular speeds of both rotary table ω_t and drill-bit ω_b have significant fluctuations due to the control action, but the equilibrium of the drill-string system for constant rotation settles down at $\omega_t = \omega_b = 4.4$ at about $t = 200$. Here, it should be noted that although the proposed PD controller can effectively suppress stick-slip vibrations, the desired rotary speed for the drill-string system is $\Omega_d = 4$ which is different from our actual equilibrium, $\omega_t = \omega_b = 4.4$. Next, we will address this issue by using the path-following methods.

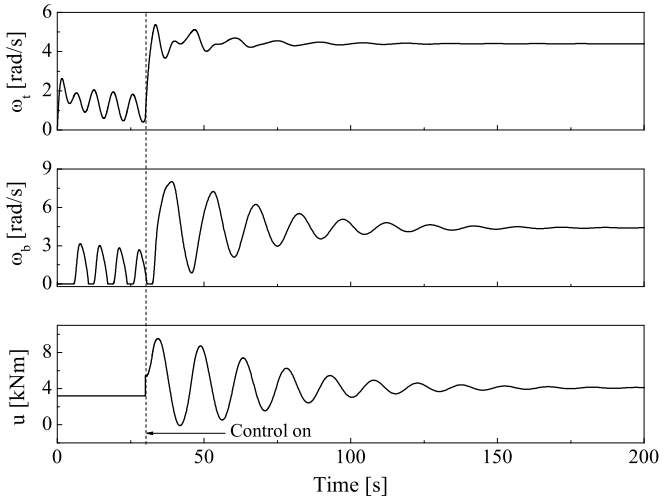

Figure 4: Dynamic response of the drill-string system for $W_b = 30$. The PD controller for which $k_1 = 500$, $k_2 = 300$, $k_3 = 200$, and $\Omega_d = 4$ is applied at $t = 30$. Stick-slip vibrations are suppressed immediately, and the rotary speed of the system settles down at $\omega_t = \omega_b = 4.4$.

One-parameter continuation of the initial stick-slip response of the drill-string model is shown in Fig. 5(e), with respect to the desired speed Ω_d (see (5)). The result is represented by the solid green curve depicted in panel (a), showing the average angular speed of the drill-bit (see (8)) on the vertical axis. Along this line the stick-slip solution remains stable and persists until the critical point GR-SL is found ($\Omega_d \approx 3.6651$), corresponding to a grazing-sliding bifurcation of limit cycles. This critical solution is plotted in panel (d), which shows a tangential intersection of the orbit with the grazing boundary $\omega_b = 0$. At the GR-SL point another branch is born (dashed, in red), which corresponds to the continuation of unstable periodic solutions with no sticking phases, as the one shown in panel (c). The grazing-sliding bifurcation found in the drill-string model (7) is characterized by a so-called non-smooth fold transition, see [29, Section 8.5.3]. This is because a branch of stable and a branch of unstable periodic solutions collide at the GR-SL point, and then disappear for parameter values above the bifurcation point.

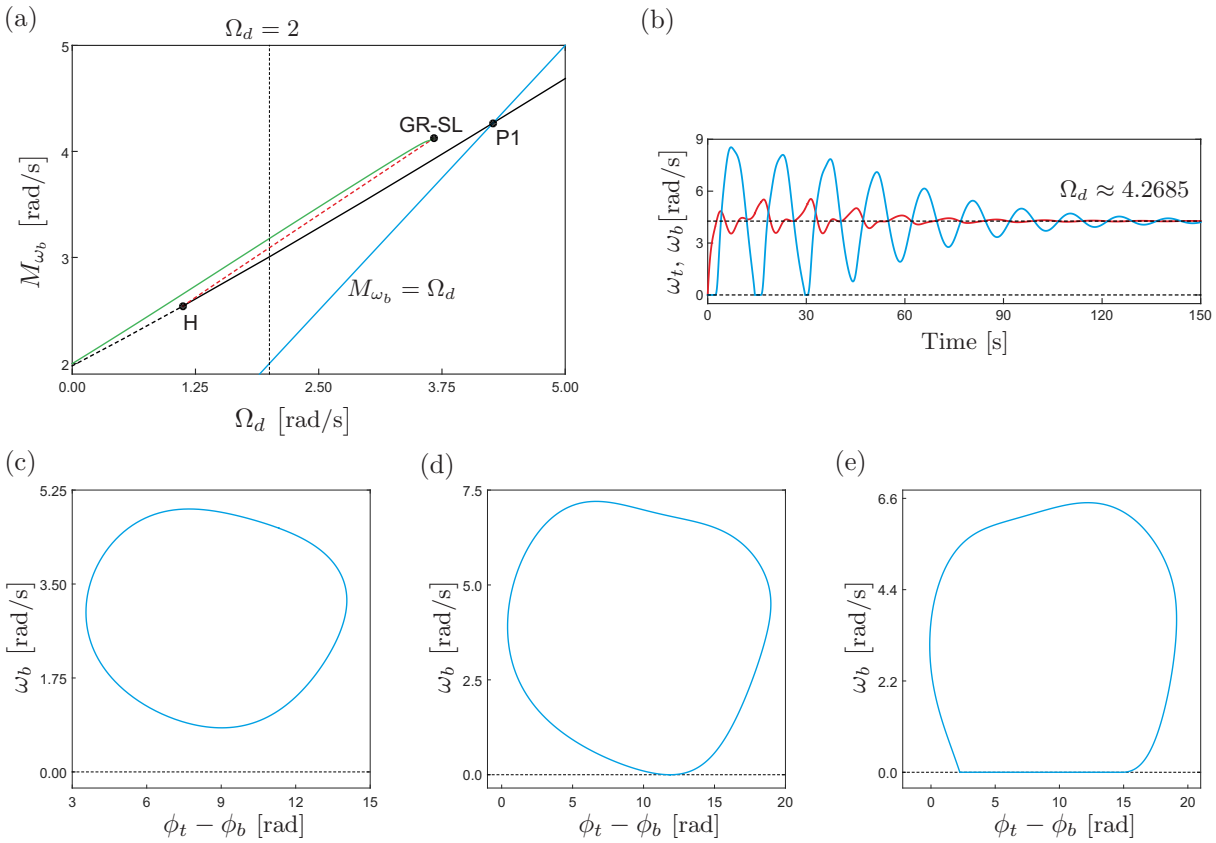

Figure 5: (a) Numerical continuation of the dynamical response of the drill-string model (7) with respect to the desired angular speed Ω_d, computed for $W_b = 30$, $k_1 = 500$, $k_2 = 300$, and $k_3 = 200$. The green and red curves represent the continuation of periodic orbits with and without stick-slip vibrations, respectively. The black line stands for the continuation of equilibrium points corresponding to constant rotation of the four disks. Along this line, the label H stands for a Hopf bifurcation. In this bifurcation diagram, solid and dashed curves represent stable and unstable solutions, respectively. The vertical axis gives the average angular speed of the drill-bit computed via (8). The blue curve represents the identity function, in such a way that the intersection at P1 gives the parameter value for which the resulting bit speed coincides with the desired speed. Panel (b) shows the system response at this point. Panels (c), (d) and (e) present phase plots for $\Omega_d = 2$ (unstable, red branch), $\Omega_d \approx 3.6651$ (grazing-sliding bifurcation GR-SL) and $\Omega_d = 2$ (stable, green branch), respectively.

Our numerical investigation reveals that the unstable periodic solutions found above are created via a subcritical Hopf bifurcation ($\Omega_d \approx 1.1177$), characterized by a positive first Lyapunov coefficient at the bifurcation point. At this point two branches of equilibria are found (black curve), one of which corresponds to stable (solid line) and the other one to unstable (dashed line) equilibrium points, respectively. Physically speaking, these points yield a system response for which all four disks rotate with a constant angular speed, and can be regarded as a desired system behaviour from a practical point of view. As the prescribed angular speed Ω_d increases, the resulting drill-bit speed M_{ω_b} increases as well, and a critical point P1 ($\Omega_d \approx 4.2686$) can be identified, where the drill bit speed coincides with the desired speed Ω_d, which can be regarded as an optimal operation point from the control perspective. This point is obtained from the intersection of the solid black curve representing stable equilibria and the blue straight line, which corresponds to the identity function $M_{\omega_b} = \Omega_d$. Panel (b) shows the system behaviour precisely at this point, where it can be seen that both the top and drill-bit angular speed settle down to the desired speed Ω_d.

By comparing Figs. 5 and 3, there are certain similarities and differences between the drill-string model with PD and open-loop torque control. One common feature is that of multistability. As mentioned earlier, under PD control the system presents a parameter window where two attractors coexist, namely, stick-slip oscillations and equilibria representing drill-bit constant rotation. In the open-loop control

scenario there appears a third attractor, corresponding to permanent sticking, which did not appear in the previous case, at least not for the considered parameter values of the PD controller. Another common feature consists in the possibility of steering the system from undesired stick-slip oscillations to equilibrium solutions with constant drill-bit rotation by suitably adjusting the considered control parameter (in this case, Ω_d and u). The main difference, however, is that the proposed PD controller allows not only the elimination of stick-slip oscillations but also a precise control of the drill-bit rotation speed, as will be analyzed and demonstrated in the next section.

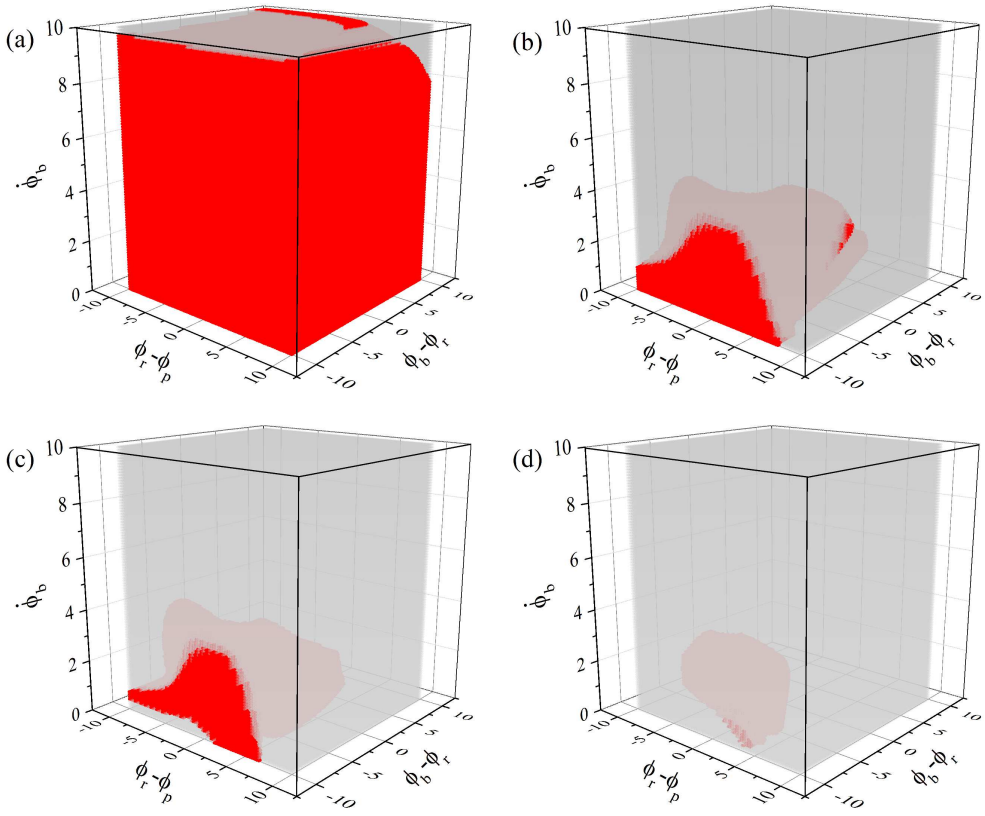

Figure 6: Basins of attraction for stick-slip vibrations (red dots) and constant rotation (grey dots) when $k_1 = 500$, $k_2 = 300$, (a) $k_3 = 300$, (b) $k_3 = 250$, (c) $k_3 = 150$, (d) $k_3 = 100$, and $\Omega_d = 2$.

Apart from the bifurcation phenomena described above, another relevant observation is the presence of coexisting attractors in the model. Specifically, there is a parameter window defined by the GR-SL and the H points found before in which two attractors coexist, namely, the stick-slip vibrations and the equilibrium solutions. Therefore, in this parameter window the system presents bistability, a feature that can be used to steer the response from a stick-slip vibration to an equilibrium with constant drill-bit rotation. Fig. 6 presents the evolution of basins of attraction of these two coexisting attractors in the coordinate $(\phi_r - \phi_p, \phi_b - \phi_r, \dot{\phi}_b)$ under variation of the control gain k_3, where the initial values that converge to stick-slip vibration and constant rotation are denoted by red and grey dots, respectively. As can be seen from Fig. 6(a), the response of stick-slip vibration dominates the initial values of the drill-string system when $k_3 = 300$. As k_3 decreases, the basin for stick-slip vibration shrinks, while the basin for constant rotation expands. This result also reveals that smaller value of k_3 will help to mitigate stick-slip vibration.

3.3. Two-parameter analysis with control

Our numerical investigation has revealed the presence of three critical points, namely, a Hopf and a grazing-sliding bifurcation, as well as a parameter value for which the desired and the actual drill-bit angular speeds coincide. In the present section we will carry out a two-parameter continuation of the critical points mentioned above in order to gain a deeper understanding of the dynamics of the drill-string model. For this purpose we will vary the desired angular speed Ω_d and the control gain k_1. The reason for choosing these parameters is because one of the main goals of the current system implementation is to set the actual drill-bit speed to the desired speed Ω_d, due to which the two last terms of the expression (5) vanish, and hence the remaining control parameter that can be effectively used is precisely k_1.

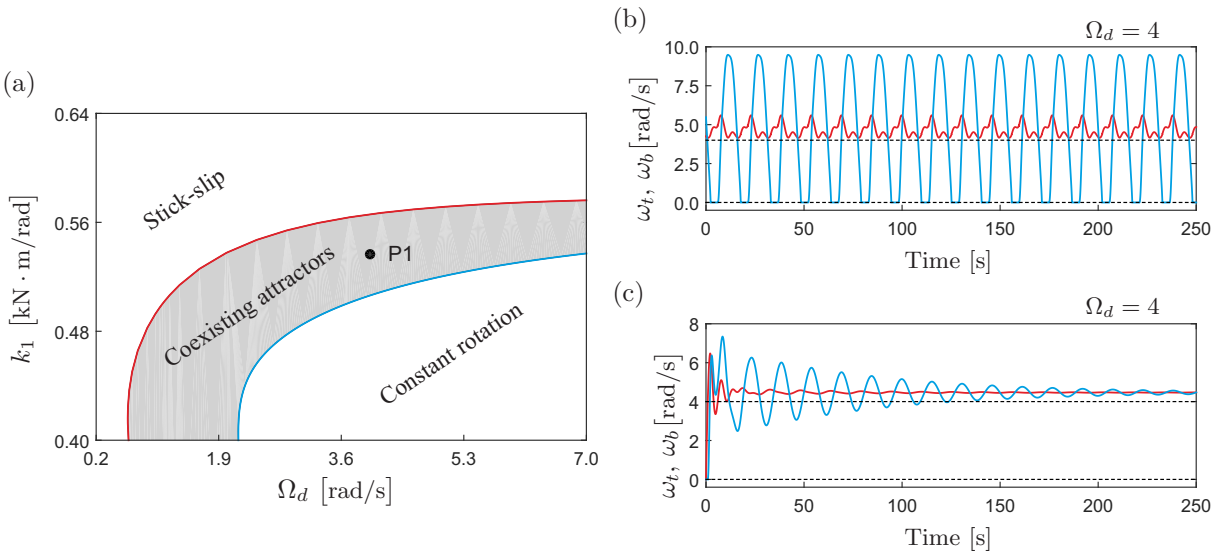

Figure 7: (a) Two-parameter continuation of the Hopf (red curve) and grazing-sliding (blue curve) bifurcations found in Fig. 5(a), with respect to the desired angular speed Ω_d and the control gain k_1. These curves define a region (grey area) in the parameter space where stable stick-slip solutions and stable equilibria (constant rotation) coexist. The area above and below the grey region yields stick-slip and equilibrium solutions, respectively. Panels (b) and (c) show coexisting stable solutions computed for P1 ($\Omega_d = 4$, $k_1 = 0.54$).

The numerical investigation begins with the two-parameter continuation of the Hopf and grazing-sliding bifurcations found in Fig. 5(a), with respect to Ω_d and k_1. The result is plotted in Fig. 7(a). This picture presents two curves corresponding to the continuation of the bifurcation points mentioned before. These curves divide the two-parameter space into three regions. The first one is located above the Hopf bifurcation curve (red) in which stable stick-slip vibrations can be found, as the one depicted in Fig. 5(e). The second region lies below the blue curve, which results from the two-parameter continuation of the grazing-sliding bifurcation of limit cycles. In this area the system presents stable equilibria which correspond to a rotation of the drill-string at a constant angular speed. The region between the red and blue curves (grey area) represents the region of bistability, a phenomenon that was already identified in the previous section. In this area, the system has, for the same set of parameters, two coexisting attractors, which are precisely the two types of system responses described above. At the test point P1 ($\Omega_d = 4$, $k_1 = 0.59$) the two coexisting solutions are computed, see Fig. 7(b) and (c).

A family of Hopf and grazing-sliding bifurcation curves for different values of WOB were presented in Fig. 8. It can be observed that the region of bistability increases as the WOB increases, and the grey area defines a common parameter region where bistability persists under varying WOB. For safe drilling with a constant rotation speed up to $W_b = 50$, the parameter region below the black grazing-sliding curve is suggested.

As can be seen from Fig. 7(b) and (c), the desired angular speed Ω_d and the resulting drill-bit speed will not necessarily be the same during the system operation. In Fig. 5(a) and (b), however, we identified an operation point for which the desired and the output speed (after transients have decayed) are exactly

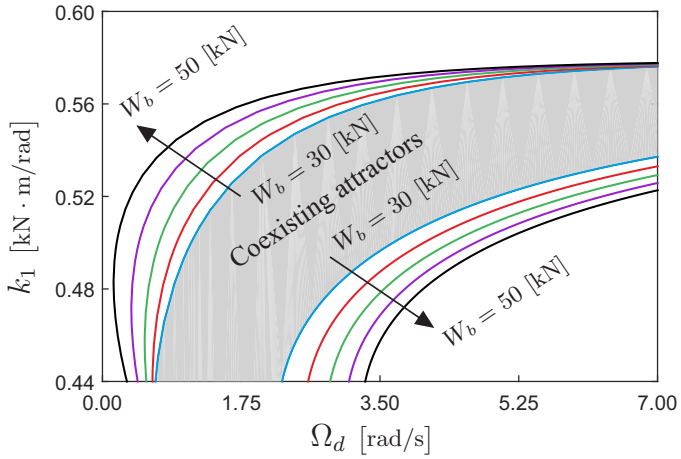

Figure 8: Family of Hopf (above the grey area) and grazing-sliding (below the grey area) curves computed for the same parameter values as in Fig. 7, and for different values of WOB, $W_b = 30$ (blue lines), $W_b = 35$ (red lines), $W_b = 40$ (green lines), $W_b = 45$ (purple lines), $W_b = 50$ (black lines). The arrow indicates the direction of increasing WOB. The grey area defines a common parameter region where bistability persists under varying WOB.

the same, and the main concern now is to determine whether the system controller is able to reproduce this ideal situation for a certain range of the desired speed Ω_d. To do so, we will carry out a two-parameter continuation of the point P1 found in Fig. 5(a), with respect to Ω_d and the control gain k_1. The result can be seen in Fig. 9(a). The computed curve comprises all combinations of Ω_d and k_1 for which the desired and the resulting drill-bit speed are the same. Furthermore, we can identify a speed range where such control is possible, given by the parameter window $1.2929 < \Omega_d < 6.0414$. This window is determined by the presence of two supercritical Hopf bifurcations labeled H1 (lower bound) and H2 (upper bound). In addition, Fig. 9(a) shows the test points Q1, Q2 and Q3 whose corresponding system responses are depicted in panels (c), (d) and (e), respectively. Here, we can see that the system indeed settles down to an equilibrium for which the top and drill bit speeds coincide with the desired speed Ω_d, hence illustrating the effectiveness of the proposed control scheme.

Another question that arises from our investigation is whether the speed range can be extended by varying a third system parameter, which could be, for instance, the WOB W_b. Specifically, we will now carry out the two-parameter continuation shown in Fig. 9(a) for different values of WOB. The result of this computation is presented in Fig. 9(b). As in the case studied in panel (a), the resulting curves define a certain parameter window where the speed control can be effectively applied. Once again, the boundaries of the parameter ranges are defined by supercritical Hopf bifurcations, represented in the picture by dots. The picture also reveals that the size of the parameter window can indeed be controlled by the WOB W_b. According to our investigation, there is a clear relation indicating that the larger W_b, the wider the speed range, which shows a remarkable interplay between the desired speed, the controller and the WOB.

In order to evaluate the contribution of the control signal employed to drive the drill-string system to the desired speed, a family of curves showing the power of the control signal (9) computed along the curves shown in Fig. 9(b) are presented in Fig. 10. As can be seen from this figure, the required power increases as the WOB increases, and faster desired speed requires more power to drive. Hence, it suggests us always to use a low WOB for a slow desired speed, while to increase the WOB accordingly as the desired speed increases.

3.4. Stick-slip severity

To test the effectiveness of the control gain of the PD controller, the stick-slip severity factor S_{ss} under variations of the WOB and the desired angular speed for different k_2 are presented in Fig. 11. Comparing the stick-slip severity factors for different k_2, it can be found that the controllable (blue) regions are similar, i.e. increasing k_2 does not improve the stick-slip severity of the system when the

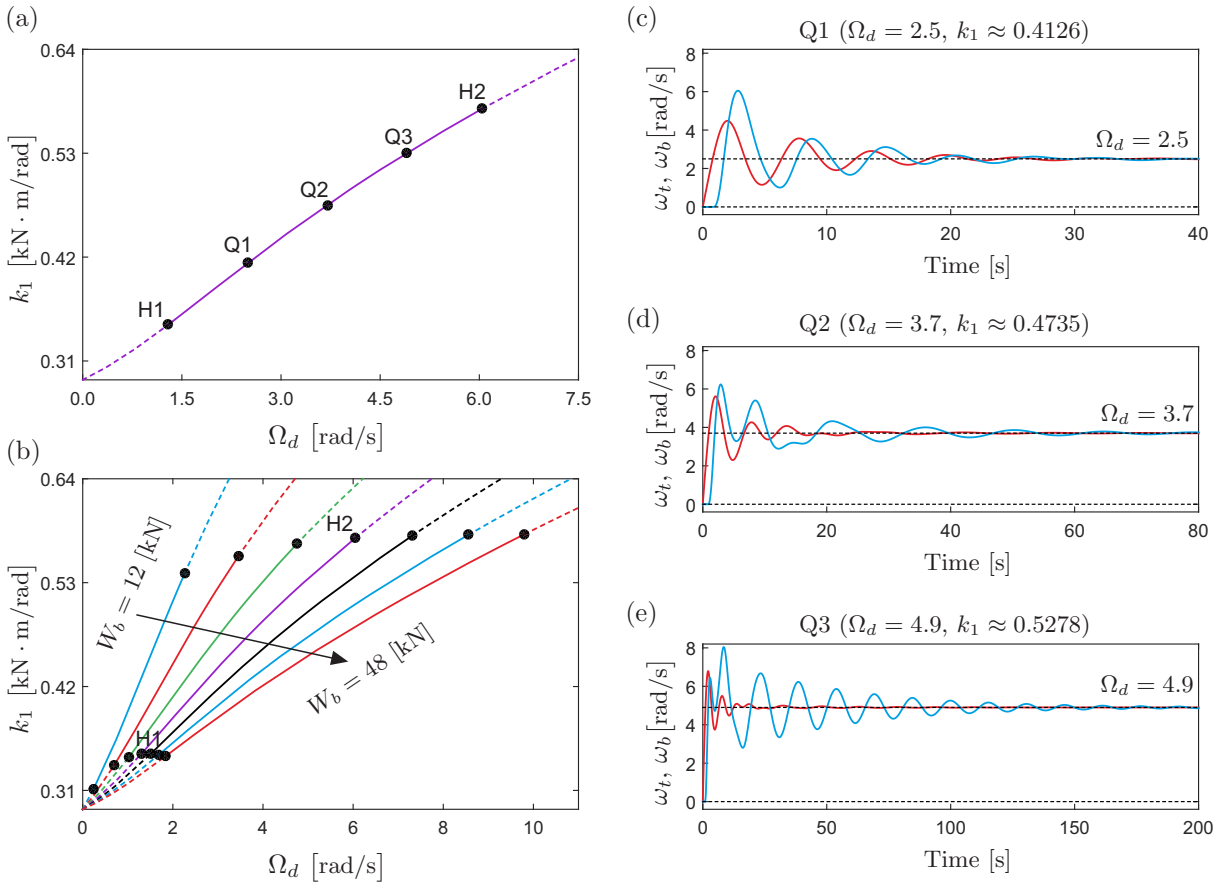

Figure 9: Panel (b) presents a family of curves (as that in panel (a)) computed for different values of WOB, $W_b = 12$, $W_b = 18$, $W_b = 24$, $W_b = 30$, $W_b = 36$, $W_b = 42$, $W_b = 48$. The arrow indicates the direction of increasing W_b. Panels (c), (d) and (e) present system responses computed at the test points Q1, Q2 and Q3, respectively, shown in panel (a).

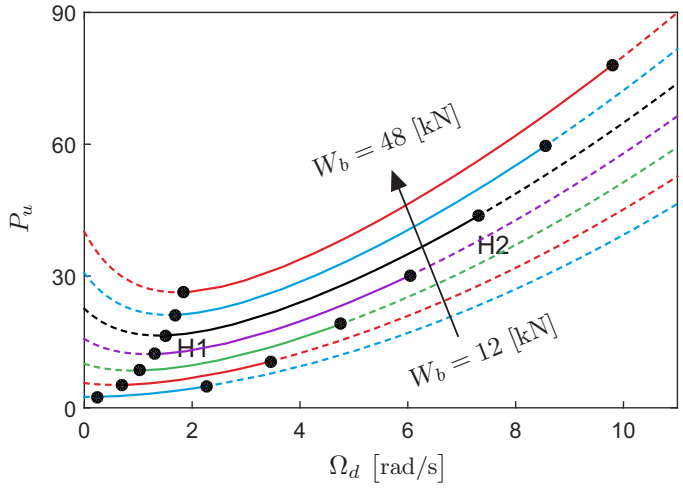

Figure 10: Family of curves showing the power of the control signal (9) computed along the curves shown in Fig. 9(b).

desired angular speed is small and the WOB is large. The dynamic responses of the drill-string system under various WOB when $k_1 = 500$, $k_2 = 300$, $k_3 = 200$, and $\Omega_d = 1.5$ are shown in Fig. 12, where the responses under various severity factors are presented. It can be seen that increasing WOB will aggravate

stick-slip severity, and the controller is only effective at $W_b = 25$ where the system is settled down to $\omega_t = \omega_b = 2.45$.

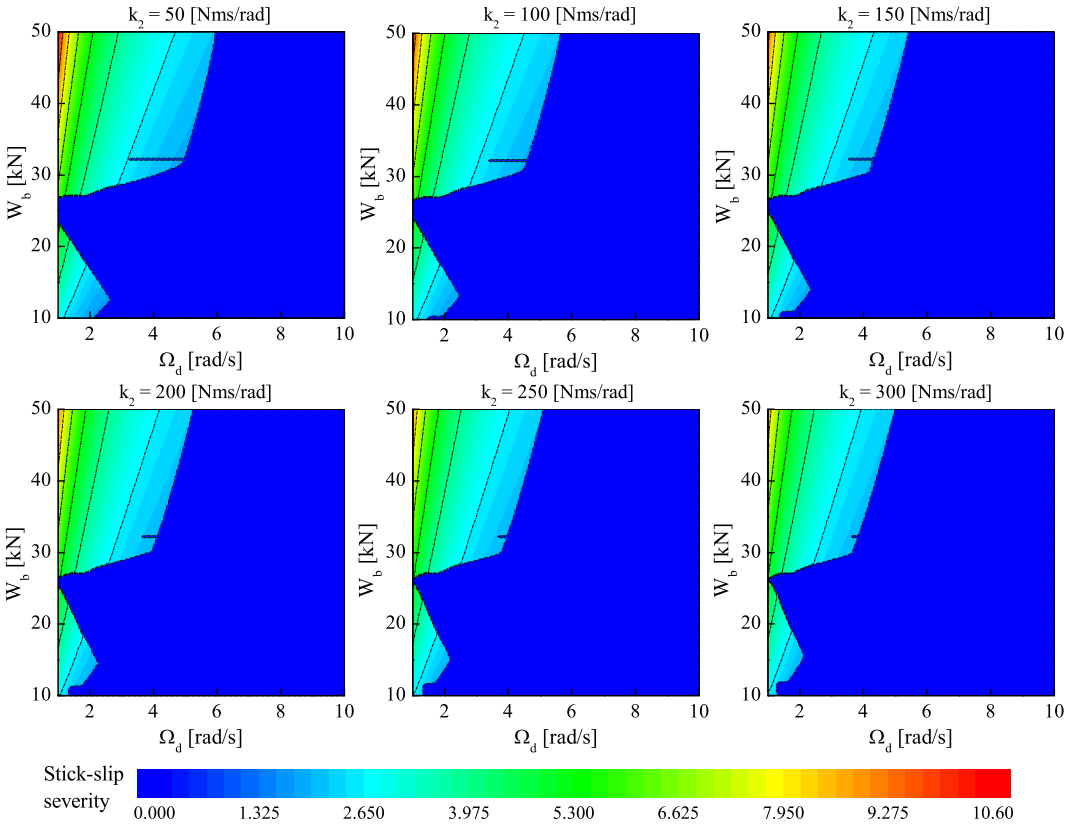

Figure 11: The effect of k_2 on stick-slip severity and controllable region (the blue areas where $S_{ss} = 0$) when $k_1 = 500$ and $k_3 = 200$.

The influence of the control gain k_3 is studied in Fig. 13 where the stick-slip severity factors under variations of the WOB and the desired angular speed are calculated. It can be seen clearly that reducing k_3 can improve the controllable region of the system, e.g. for $k_3 = 50$, the drill-string system will exhibit stick-slip vibrations for $\Omega_d < 2$ once $W_b > 30$. As the control gain k_3 increases, the stick-slip severity of the system increases and the controllable (blue) region shrinks significantly.

The reasons that k_2 has less but k_3 has significant effects on stick-slip mitigation are given as follows. Based on the controller in Eq. (5), k_2 governs the weighting of the difference between the desired rotary speed and the actual speed of rotary table, while k_3 manages the weighting of the difference between the desired rotary speed and the actual drill-bit speed. Since the stick-slip vibration emerges from drill-bit and is transferred to rotary table through drill-strings, the terms with k_3 has larger fluctuation than the one with k_2. So, the drill-string system is more sensitive to k_3. If k_3 is large, the controller takes more weighting on bit fluctuation leading to large fluctuation in control torque, which cannot help stick-slip mitigation. In addition, the term with k_2 only deals with the difference for rotary table, so regulation of this term cannot guarantee the mitigation of stick-slip vibration. However, involvement of this term is necessary as we need to regulate all the degrees of freedom of the drill-string system to the desired rotary speed.

The influence of the control gain k_1 is presented in Fig. 14 where the stick-slip severity factors under variations of the WOB and the desired angular speed are calculated. It can be seen from the figure that reducing k_1 can improve the controllable region of the system, and only small-amplitude fluctuations in rotary speed are observed (light blue areas) when $k_1 = 200$. As the control gain k_1 increases, the stick-slip severity of the system becomes worse and the uncontrollable region grows quickly. Again, if

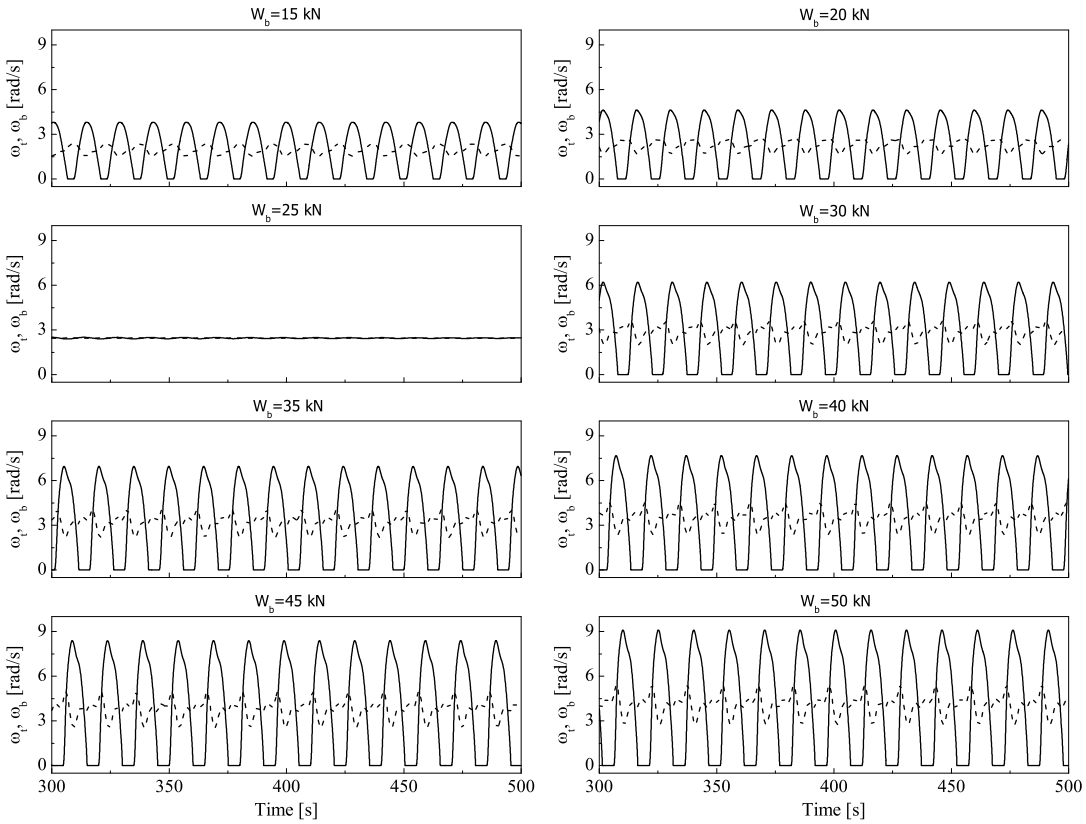

Figure 12: Time histories of rotary speeds of the rotary table, ω_t (dash lines) and the drill bit, ω_b (solid lines) under various WOB when $k_1 = 500$, $k_2 = 300$, $k_3 = 200$, and $\Omega_d = 1.5$.

k_1 is large, as it involves the difference between the rotary table and the bit speeds, the controller takes more weighting on bit fluctuation, which could cause large fluctuation in control torque. Therefore, large k_1 may aggravate the stick-slip vibrations.

4. Conclusions

This paper presents a numerical study of stick-slip mitigation and speed tuning for a drill-string system by using a recently developed proportional-derivative (PD) feedback controller. As is well-known, due to the non-smooth nature of the drill-strings induced by bit-rock interaction, the minimum controllable desired rotary speed is, in general, unknown. Secondly, the coexistence of constant rotation, stick-slip vibration, and bit sticking, has been observed at a certain parameter window of the drill-string system, as observed in our investigation. If, for instance, the system operates according to an equilibrium solution with constant rotation (which can be identified as a desirable response), a sufficiently large perturbation can switch the system to permanent bit sticking or stick-slip vibrations. In order to address these two issues, we proposed a PD feedback controller which simply adopted the relative displacement and speed between the rotary table and the drill-bit, and our studies mainly focused on exploring its capability of mitigating stick-slip vibrations and tracking the desired rotary speed, which are the main contributions of this paper.

Our one-parameter analysis shows that although the controller can effectively mitigate stick-slip vibrations, there is always a difference between the desired and the actual rotary speeds. To investigate the multistability and the speed tuning issues, we applied numerical continuation methods by following the stick-slip and the constant rotation solutions which are limited by a grazing-sliding and a Hopf bifurcation, respectively. It was observed that there was a parameter window defined by the grazing-sliding

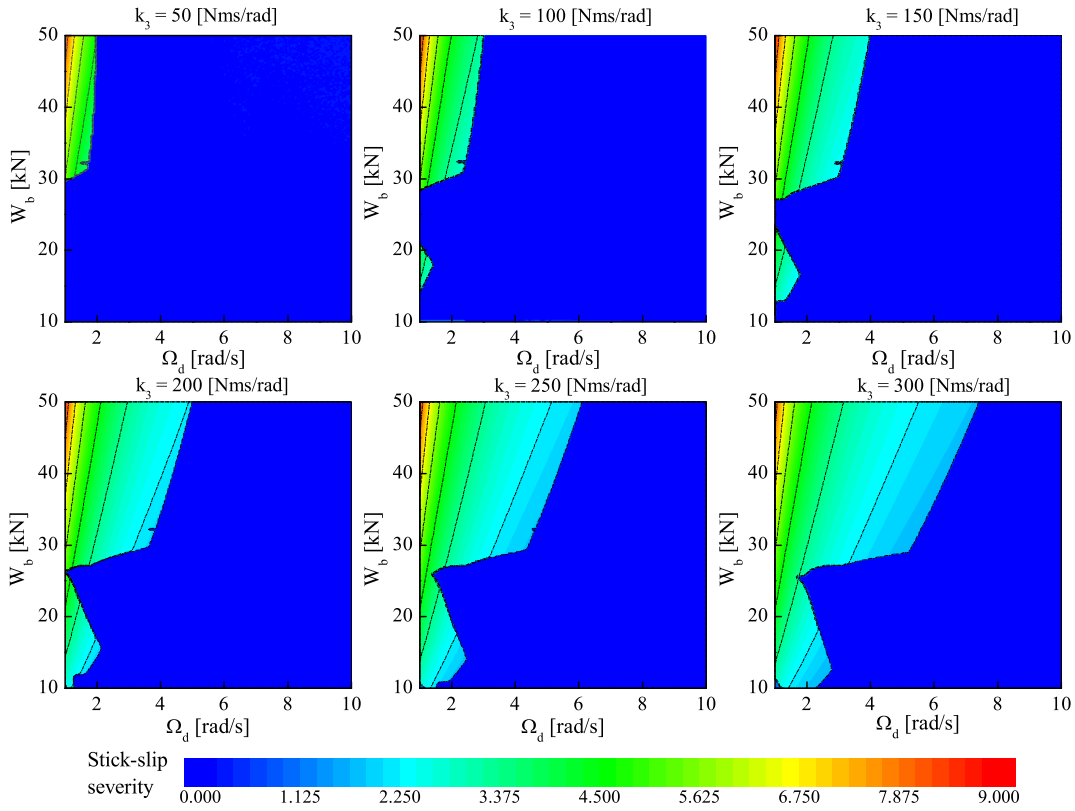

Figure 13: The effect of k_3 on stick-slip severity and controllable region (the blue areas where $S_{ss} = 0$) when $k_1 = 500$ and $k_2 = 300$.

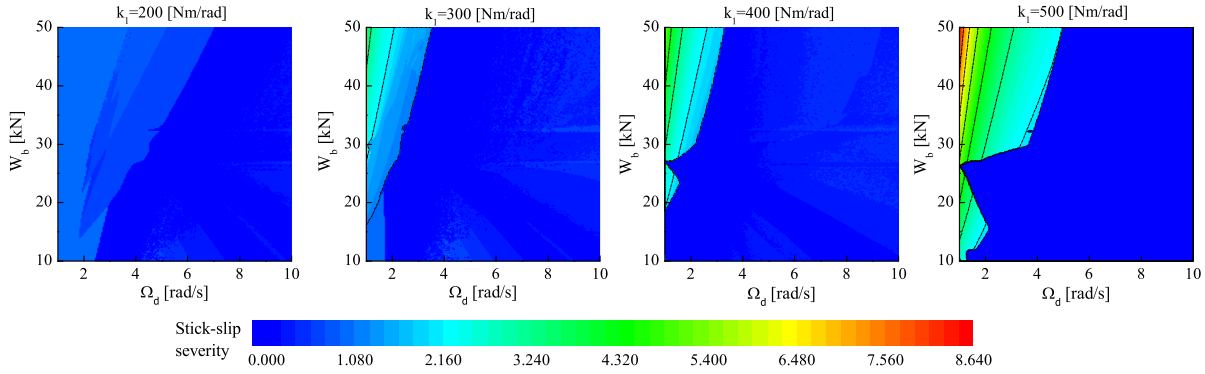

Figure 14: The effect of k_1 on stick-slip severity and controllable region (the blue areas where $S_{ss} = 0$) when $k_2 = 300$ and $k_3 = 200$.

and the Hopf points for which two attractors, stick-slip vibration and constant rotation, coexisted. This could explain the reason for the sudden emergence of the triangular blue region in the stick-slip severity window in our later analysis.

Following the one-parameter analysis, we carried out a two-parameter continuation of the grazing-sliding and the Hopf bifurcations with respect to the desired rotary speed and the control gain k_1, and the region of bistability between the Hopf and the grazing-sliding curves, i.e. the coexistence of stick-slip vibration and constant rotation, was identified. By varying the WOB, a family of these Hopf and

grazing-sliding curves were computed. Therefore, by using these curves, we can determine the minimum desired rotary speed for the proposed PD controller under different values of WOB.

To improve the tracking accuracy of our proposed PD controller, we identified an operation point for which the desired and the output speeds were exactly the same. Then, via the two-parameter continuation of this critical point with respect to the desired speed and the control gain k_1, we could identify a speed range where such control is possible, defined by the parameter window limited by two supercritical Hopf bifurcations. Within this range, we demonstrated that the drill-string system indeed settled down to an equilibrium for which the rotary and the drill-bit speeds coincided with the desired speed. Then, we computed a family of these curves for different WOBs, and found that the size of the parameter window can indeed be controlled by the WOB, showing that the larger WOB is, the wider the speed range is.

Finally, the effectiveness of the PD controller was evaluated using the stick-slip severity factor under variations of WOB and the desired rotary speed. Our calculations show that increasing the control gain k_2 does not improve the stick-slip severity of the system when the desired angular speed is small and WOB is high, while reducing the gains k_1 and k_3 can improve its controllable region significantly. Based on this investigation, future work can be focused on experimental studies of multistability in drill-strings, as well as implementation and calibration of the proposed PD controller for real applications.

Acknowledgements. This work was supported by EPSRC grant no. EP/P023983/1 and was partially supported by the National Natural Science Foundation of China grant no. 11672257 and 11872147. The first author would like to acknowledge the financial support from the China Scholarship Council (Award no. 201708510133) for his one year visiting study at the University of Exeter. The second author has been supported by the DAAD Visiting Professorships programme at the University of Koblenz-Landau.

Compliance with ethical standards.

Conflict of interest. The authors declare that they have no conflict of interest concerning the publication of this manuscript.

Data accessibility. The datasets generated and analysed during the current study are available from the corresponding author on reasonable request.

References

[1] M. Kapitaniak, V. V. Hamaneh, J. Páez Chávez, K. Nandakumar, M. Wiercigroch, Unveiling complexity of drill–string vibrations: Experiments and modelling, International Journal of Mechanical Sciences 101 (2015) 324–337.

[2] T. Richard, C. Germay, E. Detournay, A simplified model to explore the root cause of stick–slip vibrations in drilling systems with drag bits, Journal of sound and vibration 305 (3) (2007) 432–456.

[3] C. Germay, N. Van de Wouw, H. Nijmeijer, R. Sepulchre, Nonlinear drillstring dynamics analysis, SIAM Journal on Applied Dynamical Systems 8 (2) (2009) 527–553.

[4] Y. Liu, J. Páez Chávez, R. De Sa, S. Walker, Numerical and experimental studies of stick–slip oscillations in drill-strings, Nonlinear Dynamics 90 (4) (2017) 2959–2978.

[5] J. Brett, The genesis of torsional drillstring vibrations, SPE Drill Eng (1992) 168–174.

[6] Y. Liu, W. Lin, J. Páez Chávez, R. De Sa, Torsional stick-slip vibrations and multistability in drill-strings, Applied Mathematical Modelling 76 (4) (2019) 545–557.

[7] X. Liu, N. Vlajic, X. Long, G. Meng, B. Balachandran, Nonlinear motions of a flexible rotor with a drill bit: stick-slip and delay effects, Nonlinear Dynamics 72 (1-2) (2013) 61–77.

[8] P. A. Patil, C. Teodoriu, A comparative review of modelling and controlling torsional vibrations and experimentation using laboratory setups, Journal of Petroleum Science and Engineering 112 (2013) 227–238.

[9] A. Ghasemloonia, D. G. Rideout, S. D. Butt, A review of drillstring vibration modeling and suppression methods, Journal of Petroleum Science and Engineering 131 (2015) 150–164.

[10] M. Wiercigroch, K. Nandakumar, L. Pei, M. Kapitaniak, V. Vaziri, State dependent delayed drillstring vibration: Theory, experiments and new model, Procedia IUTAM 22 (2017) 39–50.

[11] F. Real, F. Fontanela, T. Ritto, A. Batou, C. Desceliers, A probabilistic model of uncertainties in the substructures and interfaces of a dynamical system: application to the torsional vibration of a drill-string, Archive of Applied Mechanics 87 (4) (2017) 685–698.

[12] R. Lima, R. Sampaio, Parametric analysis of the statistical model of the stick-slip process, Journal of Sound and Vibration 397 (2017) 141–151.

[13] X. Zhu, L. Tang, Q. Yang, A literature review of approaches for stick-slip vibration suppression in oilwell drillstring, Advances in Mechanical Engineering 6 (2014) 967952.

[14] G. Pelfrene, H. Sellami, L. Gerbaud, et al., Mitigating stick-slip in deep drilling based on optimization of pdc bit design, in: SPE/IADC Drilling Conference and Exhibition, Society of Petroleum Engineers, 2011.

[15] L. Hu, A. Palazzolo, M. Karkoub, Suppression of lateral and torsional stick–slip vibrations of drillstrings with impact and torsional dampers, Journal of Vibration and Acoustics 138 (5) (2016) 051013.

[16] K. S. Selnes, C. C. Clemmensen, N. Reimers, et al., Drilling difficult formations efficiently with the use of an antistall tool, in: IADC/SPE Drilling Conference, Society of Petroleum Engineers, 2008.

[17] C. Canudas-de Wit, F. R. Rubio, M. A. Corchero, D-oskil: A new mechanism for controlling stick-slip oscillations in oil well drillstrings, IEEE Transactions on Control Systems Technology 16 (6) (2008) 1177–1191.

[18] E. M. Navarro-López, E. Licéaga-Castro, Non-desired transitions and sliding-mode control of a multi-DOF mechanical system with stick-slip oscillations, Chaos, Solitons & Fractals 41 (4) (2009) 2035–2044.

[19] E. J. Doedel, A. R. Champneys, T. F. Fairgrieve, Y. A. Kuznetsov, B. Sandstede, X.-J. Wang, Auto97: Continuation and bifurcation software for ordinary differential equations (with HomCont), Computer Science, Concordia University, Montreal, Canada, available at `http://cmvl.cs.concordia.ca` (1997).

[20] H. Dankowicz, F. Schilder, An extended continuation problem for bifurcation analysis in the presence of constraints, Journal of Computational and Nonlinear Dynamics 6 (3) (2011) 031003.

[21] H. Dankowicz, F. Schilder, Recipes for continuation, Vol. 11, SIAM, 2013.

[22] Y. Liu, Suppressing stick-slip oscillations in underactuated multibody drill-strings with parametric uncertainties using sliding-mode control, IET Control Theory & Applications 9 (1) (2014) 91–102.

[23] M. Karkoub, M. Zribi, L. Elchaar, L. Lamont, Robust μ-synthesis controllers for suppressing stick-slip induced vibrations in oil well drill strings, Multibody System Dynamics 23 (2) (2010) 191–207.

[24] T. G. Ritto, M. Ghandchi-Tehrani, Active control of stick-slip torsional vibrations in drill-strings, Journal of Vibration and Control 25 (1) (2019) 194–202.

[25] T. Vromen, N. Van De Wouw, A. Doris, P. Astrid, H. Nijmeijer, Nonlinear output-feedback control of torsional vibrations in drilling systems, International Journal of Robust and Nonlinear Control 27 (17) (2017) 3659–3684.

[26] T. Vromen, C.-H. Dai, N. van de Wouw, T. Oomen, P. Astrid, A. Doris, H. Nijmeijer, Mitigation of torsional vibrations in drilling systems: A robust control approach, IEEE Transactions on Control Systems Technology 27 (1) (2019) 249–265.

[27] G. Leonov, N. Kuznetsov, M. Kiseleva, E. Solovyeva, A. Zaretskiy, Hidden oscillations in mathematical model of drilling system actuated by induction motor with a wound rotor, Nonlinear Dynamics 77 (1-2) (2014) 277–288.

[28] Y. Liu, J. Páez Chávez, Controlling coexisting attractors of an impacting system via linear augmentation, Physica D: Nonlinear Phenomena 348 (2017) 1–11.

[29] M. Bernardo, C. Budd, A. R. Champneys, P. Kowalczyk, Piecewise-smooth dynamical systems: theory and applications, Vol. 163, Springer Science & Business Media, 2008.